ELSEVIER

Earth and Planetary Science Letters 198 (2002) 355–369

EPSL

www.elsevier.com/locate/epsl

Osmium isotope binary mixing arrays in arc volcanism

Sophie Alves *, Pierre Schiano [1], Françoise Capmas, Claude J. Allègre

Laboratoire de Géochimie et Cosmochimie, Institut de Physique du Globe de Paris, 4 place Jussieu, 75252 Paris Cedex 05, France

Received 17 July 2001; accepted 6 February 2002

Abstract

Os isotope ratios and Os and Re concentrations were measured in 56 lavas coming from 10 different subduction zones. Samples span a large range of major element concentrations (from basalts to dacites) and Mg# (from 0.32 to 0.81). The 10 subduction zones, namely the Lesser Antilles, Java, Papua New Guinea, the Philippines, Izu–Bonin, Kamchatka, the Aleutians, Mexico, Colombia and Peru–Chile, have a range of geodynamic settings. Measured $^{187}Os/^{188}Os$ ratios range from 0.130 to 1.524 and Os concentrations range from 0.05 to 46 ppt. Re concentrations range from 24 to 915 ppt. Os initial isotope ratios are systematically positively and linearly correlated with the inverse of Os concentrations in arc lavas from a given volcano, indicating that the Os isotopic compositions always reflect a binary mixing process. Similar mixing relationships are also seen at the sample scale. All trends converge towards unradiogenic compositions similar to those of upper mantle peridotites. These mixing relationships might be ascribed to a general contamination process; however, a single shallow-level process of crustal assimilation is hardly reconciled with the diversity of basements (from oceanic crust to continental crust compositions) of the selected arc volcanoes, the occurrence of the mixing lines for both primary and differentiated samples, and the absence of covariations between Os contents, isotope ratios, and indices of contamination and differentiation. On the other hand, because subducted components are very radiogenic and differ from one zone to another, the radiogenic components may be explained by varying amounts and natures of oceanic crust and sediments in the source of arc lavas. However, this explanation implies two disequilibrium processes, first during magma formation in order to produce heterogeneous lavas, and second during magma ascent to the surface to preserve slab signatures.

Keywords: subduction; lava; osmium; crust; recycling; mixing; rhenium; isotope ratios

* Corresponding author. Present address: Pheasant Memorial Laboratory, Institute for Study of the Earth's Interior, Okayama University at Misasa, Misasa, Tottori-Ken 682-0193, Japan. Tel.: +81-858-43-3826; Fax: +81-858-43-3795.

E-mail addresses: salves@pheasant.misasa.okayama-u.ac.jp (S. Alves), schiano@opgc.univ-bpclermont.fr (P. Schiano), capmas@ipgp.jussieu.fr (F. Capmas), allegre@ipgp.jussieu.fr (C.J. Allègre).

[1] Present address: Laboratoire Magmas et Volcans, Université Blaise-Pascal, 5 rue Kessler, 63038 Clermont-Ferrand Cedex, France.

0012-821X/02/$ – see front matter
PII: S0012-821X(02)00524-1

1. Introduction

Isotopic and geochemical studies on subduction-related lavas aim at constraining the nature of their mantle sources and the role of source heterogeneity and petrogenetic processes in their compositions. Many components are potentially involved in producing the geochemical signatures of arc lavas: depleted mantle, subducted materials, and arc basements. Moreover, the components involved contribute by complex mixing of their fluid and melt derivatives.

Isotopic tracers are particularly suitable to study the sources of arc magmas (e.g., [1]). U/Th disequilibria and boron systematics suggest an oceanic crust fluid influence for most convergent margins (e.g., [2,3]), and contribution of subducted sediments is largely recognized in strontium, neodymium and lead signatures of arc lavas (e.g., [1]).

The Re–Os isotopic system has previously been used to assess recycled basaltic materials in mantle sources of ocean island basalts (OIB), mid-ocean ridge basalts (MORB) (e.g., [4–6]), and arc lavas [7]. Here, we undertook a systematic study of Re–Os isotopic characteristics of arc lavas for various subduction zones all over the world. Os isotope ratios are potential tracers of slab contribution in arc lavas because: (1) subducted sediments are very radiogenic in Os compared to the upper mantle (e.g., [8]), and (2) Re behaves as a moderately incompatible element during mantle partial melting, whereas Os is highly compatible. Therefore, MORB have much higher Re/Os ratios than peridotites ($^{187}Re/^{188}Os = 140–16\,000$ for MORB [6], $^{187}Re/^{188}Os \approx 0.5$ for peridotites (e.g., [9])). Consequently, old oceanic crust is likely to be extremely more radiogenic than the depleted upper mantle, so that recycled basaltic components should be identified by their elevated $^{187}Os/^{188}Os$ ratios.

However, crustal materials are also likely to be rather radiogenic in osmium (e.g., [10]), and contamination via assimilation of the arc basement is a potential way to impart high Os isotopic signatures to arc magmas and consequently mask the source signatures acquired in the mantle melting zone.

Arc lavas may have very low Os concentrations (as low as <1 ppt [7]) and so far this characteristic has been an important limitation for their analysis. Yet, an increasing number of studies on arc lava Os isotope characteristics [7,11,12] show very radiogenic osmium signatures, which are interpreted in terms of either mantle source heterogeneity [7,11] or secondary crustal contamination [11,12].

We present Os and Re concentrations and isotope ratio data for 56 arc lavas from 10 subduction zones selected to represent a wide range of geodynamic characteristics, and the results are discussed in terms of the two mentioned hypotheses: potential magma sources or contaminants.

2. Geological background

Physical parameters of the 10 subduction zones selected for the study are presented in Table 1 and summarized here. Subducted oceanic crust ranges from 15 to 150 Ma, sediment thickness of the accretionary prism varies from 125 to 1750 m and crustal basements of the arcs are 15–70 km thick. The nature of basements also varies from one zone to another, with mafic (Java), basaltic (Aleutians, Lesser Antilles), accreted arc terrane type (Kamchatka) and continental crust (Central and South America) compositions. For most of the samples, stratigraphic or absolute K–Ar ages are known and are less than a few hundred kyr (cf. Table 2). Moreover, samples from a given volcano span a limited range of ages.

For some of the arcs (Lesser Antilles, Izu–Bonin, Kamchatka, Aleutians, and Mexico), we measured Os contents and isotope ratios for several samples of the same volcano (Table 2). For 35 of these 39 samples, major and trace element data were obtained at CRPG Nancy (SiO_2, Mg# and Ni are given in Table 2). The samples span a large range of major element concentrations, mainly in the calc-alkaline series, from basalts to dacites, and all show normalized trace element patterns typical for subduction-related magmatism (Fig. 1). Kamchatka (51–55 wt% SiO_2, Mg# 0.52–0.81) and the Lesser Antilles (49–62 wt% SiO_2, Mg# 0.46–0.68) samples are mostly

Table 1
Geophysical characteristics of the 10 subduction zones

Subduction zone	Convergence rate[a] (cm/yr)	Age of AOC[b] (Ma)	Sediment thickness on the AOC[c] (m)	Basement thickness[e] (km)	Crustal basement geochemical nature[f]
Lesser Antilles: North/South	1.4	86/100–150	235/1750	25/30–35	Oceanic
Java	7.6–7.9	138	300	25–30	Mafic/ultramafic rocks+Sediments[g]
Papua New Guinea	9–14	50	1500[d]	30	Oceanic
Philippines	9	50	120	–	Transitional
Izu–Bonin (oceanic arc/Fuji)	9.6–6.7	146	600	15–18/30	Oceanic/continental[h]
Kamchatka	8.9–9.2	90	364	25–45	Accreted arc terranes +obducted oceanic crust[i]
Aleutians	8.7–7.0	54	350	18–25	Oceanic
Mexico	5.7–8.5	15	170	30	Continental
Colombia	8.9–8.4	15	270	66	Continental
Peru–Chile	10.3–10.8	26–82	125	40–70	Continental

[a] [34], except for Papua New Guinea [35] and Philippines [36].
[b] AOC: altered oceanic crust [37], except for Lesser Antilles [38].
[c] [36].
[d] [39].
[e] [34], except for Papua New Guinea [40] and for Northern Lesser Antilles [30].
[f] [37] unless specified.
[g] [41].
[h] [42].
[i] [43].

undifferentiated to slightly differentiated basalts and andesites, whereas most of the rocks from Izu–Bonin (49–66 wt% SiO_2, Mg# 0.39–0.63) and the Aleutians (46–61 wt% SiO_2, Mg# 0.35–0.54) are differentiated with basaltic to dacitic compositions (cf. Table 2).

3. Analytical techniques and results

Os and Re were extracted using the chemical separation previously described by J.-L. Birck et al. [13]. This low blank Os extraction procedure makes it possible to measure reliable Os isotope ratios in rock samples with 1 ppt or less of total Os content. For each sample 0.5–5 g of powder was used. The mean 2σ error (including propagation of blank error due to correction) of the isotopic ratios was 1.5%, with three of 90 measured ratios having an error higher than 5% (maximum 11.3%). Because of improvement of the reagent purification processes, the total Os blank decreased during the course of the study from 0.220 pg to 0.005 pg, with a mean value of 0.078 pg. The blank average contribution for Re was less than 20 pg. A total of 39 blank measurements were performed during the period of the study, which corresponds to one blank measurement for every three sample analyses. Analyses were performed by negative ion thermal ionization mass spectrometry on a Finnigan Mat 262 at IPG-Paris. Twenty-three runs of the laboratory standard solution diluted at various Os concentrations (loads of 0.5–10 pg) were performed throughout the study period. The mean $^{187}Os/^{188}Os$ ratio of the standard was 0.1742 ± 0.0002. In order to test sample homogeneity, we made duplicate analyses using different aliquots from the same batch of 30–50 g of powder made from a single piece of rock.

The concentration data for all the arc lavas analyzed are given in Table 2. Os concentrations are extremely low and variable, ranging from 0.05 to 46 ppt, and Re contents range from 24 up to 915 ppt. $^{187}Re/^{188}Os$ ratios range from 5 to 54 200. Although Os and Re contents of the samples might have been somehow affected by fractional crystallization (see Section 4), it is interesting to

Table 2
Os and Re concentrations and Os isotopic ratios for arc volcanoes

Sample[a]	Island/Volcano/ Location	Rock type	Age or date of eruption[b] (yr)	$^{187}Os/^{188}Os$ ($\pm 2\sigma$ error)[c]	Os (ppt)	Re (ppt)	$\frac{^{187}Re}{^{188}Os}$	$\frac{^{187}Os}{^{188}Os^{d}_{init}}$	SiO_2[e] (wt%)	Mg#[e]	Ni[e] (ppm)
Lesser Antilles											
SB9 I	Saba/Mt. Sceney/ Principal Dome	andesite	$\sim 10^6$	0.595 (0.004)	2.000	67	171	0.592	54.67	0.68	98
SB9 II				0.540 (0.003)	1.418	139	498	0.531			
SB7 I	Saba/Well's Bay Dome	andesite	4.20×10^5	0.957 (0.013)	0.728	188	1 376	0.948	60.6	0.59	21
SB7 II				1.450 (0.011)	0.905	164	1 023	1.443			
SB53	Saba/Old Booby's Dome	andesite	$\sim 10^6$	0.404 (0.003)	1.054	150	706	0.392	53.7	0.66	50
SB67	Saba/Airport 2nd flow	andesite	$< 5\times10^5$	0.215 (0.001)	2.090	150	350	0.212	55.8	0.68	85
SB49	Saba/Upper Hell's Gate, Ancient Dome	andesite	$\sim 10^6$	0.220 (0.002)	1.729	464	1 306	0.198	59.55	0.61	35
SK 11	St. Kitts/Mt. Misery	basalt	$< 10^4$	0.179 (0.002)	0.940	301	1 551	0.179	50.3	0.54	9
SK9 I	St. Kitts/Mt. Misery	andesite	$< 10^4$	0.407 (0.008)	0.248	184	3 763	0.407	56	0.54	12
SK9 II				0.446 (0.011)	0.241	187	3 862	0.445			
SK9 III				0.432 (0.005)	0.257	185	3 601	0.431			
SK6	St. Kitts/Mt. Misery	basalt	$< 10^4$	0.236 (0.004)	0.679	335	2 404	0.235	49	0.62	31
SK2 I	St. Kitts/Mt. Misery	andesitic basalt	$< 10^4$	0.382 (0.005)	0.519	345	3 339	0.381	53	0.52	10
SK2 II				0.560 (0.017)	0.396	361	4 611	0.559			
SK2 III				0.498 (0.003)	0.366	383	5 282	0.497			
F802	Guadeloupe/ Soufrière/Nuée St. Vincent	andesite	$1–2\times10^5$	0.266 (0.030)	1.461	357	1 199	0.262	57.21	0.48	5
F802 II				0.274 (0.003)	1.004	457	2 234	0.267			
MG 802	Martinique/Mt. Pelée	andesite	1902	0.149 (0.001)	1.911	103	262	0.149	62.04	0.46	4
MI 902 I	Martinique/Mt. Pelée, Aileron Dome	andesite	13.5×10^3	0.743 (0.005)	0.375	101	1 413	0.742	60.94	0.46	2
MI 902 II				0.811 (0.025)	0.284						
MF 902	Martinique/Mt. Pelée, Morne Plumée	andesitic basalt	$1–5\times10^5$	0.229 (0.002)	0.837	144	842	0.222	55.17	0.53	7
SV6 I	St. Vincent	andesitic basalt	1979	0.624 (0.003)	2.530	393	798	0.624	54.1	0.55	22
SV6 II				0.571 (0.004)	3.096	430	708	0.571			
SV8001 I	St. Vincent/ Soufrière	andesitic basalt	$< 6\times10^5$	0.348 (0.001)	5.631			0.348	53.48	0.54	17
SV8001 II				0.465 (0.004)	3.514	310	445	0.461			
SV8001 III				0.555 (0.002)	2.926	279	486	0.550			
Java											
MR 43 A	Java/Merapi	basalt		0.523 (0.004)	1.823	448	1 248				
BL 36 (39)	Java/Baluran	basalt		0.262 (0.002)	5.416	246	223				

Table 2 (*Continued*)

Sample[a]	Island/Volcano/ Location	Rock type	Age or date of eruption[b] (yr)	$^{187}Os/^{188}Os$ ($\pm 2\sigma$ error)[c]	Os (ppt)	Re (ppt)	$\frac{^{187}Re}{^{188}Os}$	$\frac{^{187}Os}{^{188}Os^{d}_{init}}$	SiO_2[e] (wt%)	Mg#[e]	Ni[e] (ppm)
Papua New Guinea											
94-LIH-11	Papua New Guinea/Lihir		$<1.6\times10^6$	0.1728 (0.0008)	19.60	220	54	0.1585			
94-AMB-29	Papua New Guinea/Feni/ Ambittle		$<1.6\times10^6$	0.1310 (0.0004)	38.75	37	5	0.1298			
Philippines											
KH920814-01	Pinatubo	andesite	1991	0.258 (0.003)	0.755	399	2 587	0.258			
Izu–Bonin											
YH76 I	Honshu/ Hakone	basalt	6×10^5	0.164 (0.003)	1.146	328	1 378	0.151	50.69	0.63	56
YH76 II				0.192 (0.013)	1.227	477	1 885	0.174			
YH76 III				0.162 (0.001)	1.220	312	1 239	0.150			
YH18	Honshu/ Hakone	dacite	2.7×10^5	0.831 (0.031)	0.062	384	28 884	0.703	64	0.40	2
YH18 II				1.181 (0.047)	0.048	396	54 197	0.941			
YH18 III				0.567 (0.010)	0.109	490	22 891	0.466			
K8	Honshu/ Hakone/ Komagatake	andesite	1.5×10^4	0.154 (0.002)	1.461	353	1 283	0.154	58		
No. 14 I	Izu Oshima/Mt. Mihara	andesite	1986	0.430 (0.010)	0.196	727	17 885	0.430	57.38	0.39	4
No. 14 II				0.419 (0.009)	0.205	726	18 250	0.419			
No. 14 III				0.409 (0.006)	0.284	865	15 197	0.409			
No. 28	Izu Oshima/Mt. Mihara	basalt	1986	0.161 (0.004)	0.641	433	3 230	0.161	52.7	0.46	17
No. 28 II				0.209 (0.007)	0.639	432	3 324	0.209			
OM4	Honshu/ Omuro/ Komuroyama	andesitic basalt	10^4	0.144 (0.001)	3.615	347	463	0.144	53.3		
Hino I	Honshu/Mt. Fuji/ Hinokimarubi	basalt	$<1730\pm30$	0.163 (0.002)	1.705	416	1 182	0.163	50.08	0.52	37
Hino II				0.208 (0.004)	1.446	662	2 238	0.208			
F5	Honshu/Mt. Fuji/ Aokigahara	basalt	864	0.140 (0.001)	3.425	373	525	0.140	50.41	0.52	40
1707	Honshu/Mt. Fuji/Hoei crater	dacite	1707	0.155 (0.001)	7.781	522	325	0.155	66.06	0.43	
F2	Honshu/Mt. Fuji/Mishima	basalt	2×10^5	0.165 (0.001)	5.974	132	107	0.165	48.8		
Kamchatka											
K77381 I	Klyuchevskoy	basalt	$<10^4$	0.1416 (0.0005)	10.48	387	181	0.142	51.59	0.76	211
K77381 II				0.141 (0.001)	9.581	353	178	0.141			
K56P66 I	Klyuchevskoy	andesitic basalt	1966	0.201 (0.004)	2.484	658	1 289	0.201	53.62	0.59	30
K56P66 II				0.203 (0.002)	2.186	463	1 030	0.203			
T 1475 II	Tolbachik	basalt	1975	0.175 (0.001)	8.595	409	235	0.175	50.85	0.72	112
T 1475 II				0.176 (0.001)	8.390	377	218	0.176			
PT30476 II	Tolbachik	basalt	1976	0.147 (0.001)	11.88	450	183	0.147	51.72	0.54	50
PT30476 II				0.147 (0.001)	11.15	506	217	0.147			

Table 2 (*Continued*)

Sample[a]	Island/Volcano/ Location	Rock type	Age or date of eruption[b] (yr)	$^{187}Os/^{188}Os$ ($\pm 2\sigma$ error)[c]	Os (ppt)	Re (ppt)	$\frac{^{187}Re}{^{188}Os}$	$\frac{^{187}Os}{^{188}Os^{d}_{init}}$	SiO_2[e] (wt%)	Mg#[e]	Ni[e] (ppm)
P33182 I	Tolbachik	basalt	$<10^4$	0.223 (0.005)	0.514	536	5 067	0.222	52.57	0.55	20
P33182 II				0.242 (0.006)	0.571	678	5 796	0.241			
P33182 III				0.246 (0.004)	0.624	484	3 802	0.245			
P33182 IV				0.153 (0.003)	1.400	426	1 470	0.153			
651-1 I	Krasheninnikov	andesitic basalt	3.96×10^4 (?)	0.230 (0.002)	0.311				53.14	0.54	20
651-1 II				0.210 (0.006)	0.324	680	10 312	0.203			
651-1 III				0.134 (0.003)	1.285						
651-1 IV				0.200 (0.007)	0.467	559	5 794	0.196			
A29107 I	Avachinsky	andesitic basalt	$<1.8\times10^6$	0.1366 (0.0005)	11.15	286	125	0.136	54.49	0.60	23
A29107 II				0.228 (0.008)	0.530	646	5 974	0.227			
A29107 III				0.181 (0.010)	1.090	361	1 498	0.181			
A8501[f]	Avachinsky	basalt	$<1.8\times10^6$	0.133 (0.001)	46.00				51.66	0.81	250
K80317 I	Mutnovski	basalt	$<10^4$	0.236 (0.005)	0.747	757	4 967	0.235	51.49	0.52	14
K80317 II				0.231 (0.003)	0.832	915	5 376	0.230			
Aleutians											
B 1927 I	Bogoslof	basalt	1927	0.201 (0.001)	3.763	24	31	0.201		0.53	
B 1927 II				0.319 (0.006)	1.618	166	507	0.319			
B 1796 I	Bogoslof	andesite	1796	0.136 (0.001)	5.636	537	935	0.136		0.33	
B 1796 II				0.155 (0.001)	6.979	589	408	0.155			
ADK53	Adak	andesite	1796	0.1378 (0.0005)	23.56	174	36	0.1378			
UM21 I	Umnak/Okmok	basalt	1946	0.144 (0.001)	1.364	611	2 162	0.144			
UM21 II				0.202 (0.001)	1.054	730	3 371	0.202			
Mexico											
VE21	Pico de Orizaba	andesite		0.371 (0.004)	0.672	251	1 861				
PU12	Popocatepetl/ Puebla	andesite	$<23\,000$	0.250 (0.001)	6.263	287	225	0.250			
PO1	Popocatepetl	basalt	$<23\,000$	0.289 (0.003)	4.296	179	206	0.289			
PO6	Popocatepetl	basalt	$<23\,000$	0.313 (0.004)	3.287	158	238	0.313			
SOC9301-A	Socorro Island	basalt	1993	0.130 (0.001)	3.884	710	881	0.130			
Colombia											
KH 950727	Colombia/ Galeras	andesite		0.279 (0.003)	1.647	187	559				
Peru–Chile											
SHILA I	Peru/Shila			0.521 (0.005)	1.207	170	713				
16A	Chile/Sierra del Lipez	andesite		1.524 (0.007)	2.141	100	265				
6B	Chile/Miscanti	andesite		0.770 (0.003)	1.877	176	491				
17L	Chile/Antuco	basalt	$<10\,000$	0.145 (0.003)	1.593	234	712	0.145			
18N	Chile/Villarrica	basalt	$<14\,000$	0.133 (0.001)	4.761	165	168	0.133			
19M	Argentina/El Pedrero	basalt		0.215 (0.001)	21.01	104	24				

[a] Numbers I, II, III and IV are for duplicates of the same sample.

[b] For Lesser Antilles, Kamchatka, Aleutians, Japan and Papua New Guinea, age references are respectively, R. Maury, personal communication (and [44] for SV8001), [45], [28], [46] and I. Kaneoka, personal communication and [47].

[c] Mass fractionation was corrected using $^{192}Os/^{188}Os = 3.08271$. Measured ratios were corrected for blank contribution. 2σ errors take blank error propagation into account when several blanks are available for a short period of time.

[d] Age correction uses $\lambda_{Re} = 1.64\times10^{-11}$ yr^{-1} [48].

[e] SiO_2, Mg# and Ni compositions were measured at CRPG, Nancy, France, by emission-ICP and ICP-MS respectively, except for Bogoslof [49] and Antilles (SiO_2 and Mg# from R. Maury, personal communication).

[f] Os data from [50].

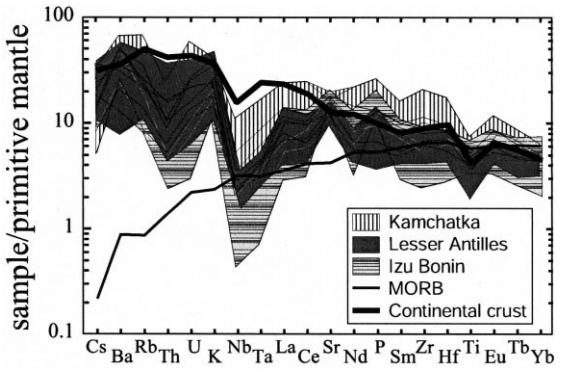

Fig. 1. Spidergram of trace element concentrations normalized to primitive mantle [32], for Izu–Bonin, Lesser Antilles and Kamchatka arcs. Gray fields show ranges for each subduction zone, and thick black lines are for MORB [32] and continental crust [33]. Note that for Kamchatka, there are no Ta data. The samples show trace element patterns typical for subduction-related magmatism, that is, enriched in large ion lithophile elements, and depleted in high field strength elements, and in heavy rare earth elements, relative to MORB.

note that all arc lavas plot on the terrestrial trend defined on the $^{187}Re/^{188}Os$ versus Os diagram (Fig. 2 and [14]).

Os isotopic compositions of arc lavas span a very large range of $^{187}Os/^{188}Os$ values, from abyssal peridotite-like ratios to extremely radiogenic values (Fig. 3). In particular, initial $^{187}Os/^{188}Os$ ratios (corrected for sample ages given in Table 2) range from 0.149 to 1.443 for the Lesser Antilles rocks, 0.140 to 0.941 for Central Japan (Izu–Bonin arc), 0.137 to 0.245 for Kamchatka, 0.136 to 0.319 for the Aleutian volcanoes, and 0.130 to 0.313 for Mexico. On average, these ratios are higher than those known for other oceanic basalts (e.g., [4–6]). Fig. 4 shows initial $^{187}Os/^{188}Os$ ratios plotted against $1/^{188}Os$ for arcs for which many samples were analyzed per volcano, including in Fig. 4f the data previously obtained for West Java [7]. In such a diagram, each volcano appears to define one positive linear correlation, or two trends for two different periods in a volcano's life (Fig. 4f). All trends have high correlation coefficients ($r^2 > 0.79$), except Saba ($r^2 = 0.60$) and St. Kitts ($r^2 = 0.41$) in the Lesser Antilles. Note, however, that if the radiogenic sample SK2, with intermediate Os concentrations, is not taken into

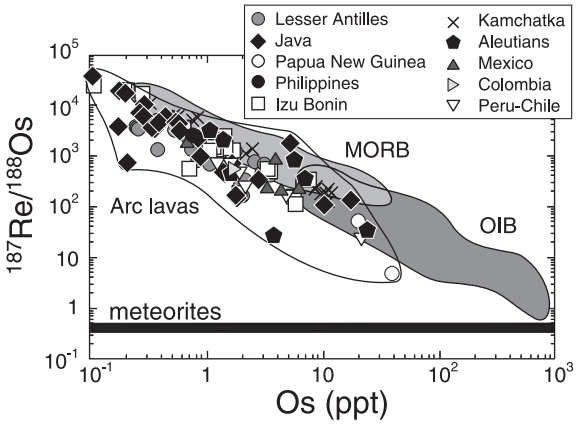

Fig. 2. $^{187}Re/^{188}Os$ ratio versus Os concentrations for arc lavas, MORB and OIB (references in the text). The meteorite trend [14] is included for comparison.

account, the regression line for St. Kitts changes to an almost parallel line with $r^2 = 0.98$ (Fig. 4).

Because the presented isotope ratios were corrected for sample ages, these relationships cannot reflect isochronal trends from the $^{187}Os/^{188}Os$ versus $^{187}Re/^{188}Os$ diagram, where the $^{187}Re/^{188}Os$ ratio would be dominated by the variations of Os contents. Instead, these linear trends must rep-

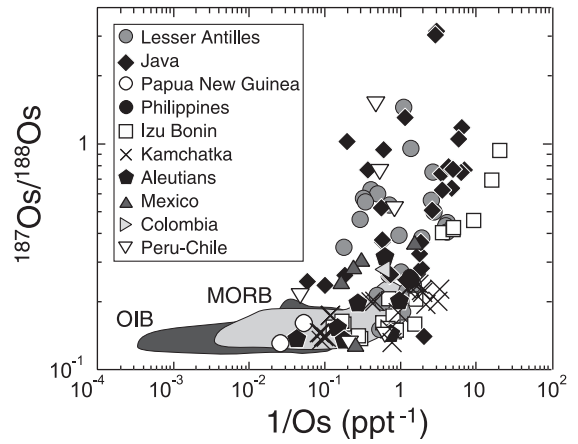

Fig. 3. Osmium isotopic ratios versus the inverse of Os concentrations in arc lavas (this study and [7]), MORB and OIB (references in the text). Except for Mexican and South American samples and two samples from Java, all isotope ratios are corrected for post-eruption Re radio-decay according to ages given in Table 2. Note that for South American samples with no known age, the $^{187}Re/^{188}Os$ are relatively low (compared to the whole set of data) and therefore, the age correction would probably not greatly change the isotope ratio.

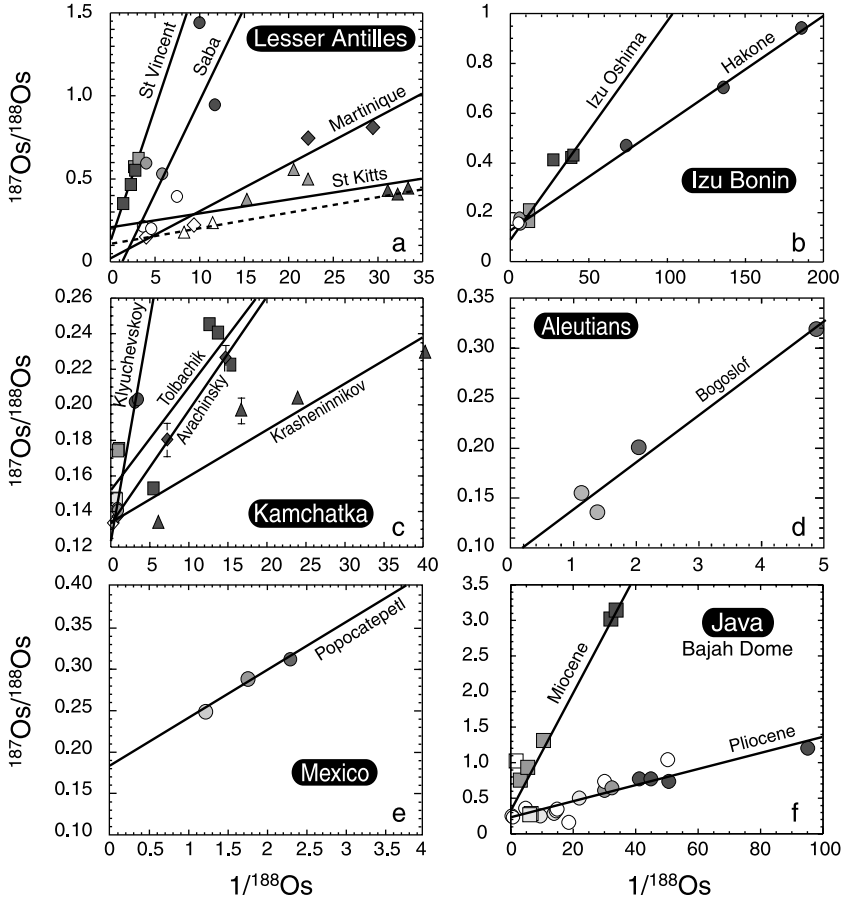

Fig. 4. $^{187}Os/^{188}Os$ versus $1/^{188}Os$ diagrams for the Lesser Antilles (a), Izu–Bonin (b), Kamchatka (c), the Aleutians (d), Mexico (e) and West Java [7] (f). Each volcano is represented by one single shape of symbol. White symbols are for samples analyzed once and shades of gray are for multiple analyses of one given sample (for example the three dark gray circles in b are for three analyses of the Hakone YH18 sample). When larger than the symbol, error bars are added for isotope ratios. Each volcano displays one alignment, for which the regression line is shown. The intercept values (i) and correlation coefficients (r^2) of these regression lines are as follows ($i-r^2$): St. Vincent (0.128–0.96); Saba (−0.132–0.60); Martinique (0.013–0.96); St. Kitts (0.210–0.40) or (0.108–0.98) (dotted line if sample SK2 is not considered, see text); Izu Oshima (0.093–0.89); Hakone (0.130–0.998); Klyuchevskoy (0.123–0.99); Tolbachik (0.153–0.79); Avachinsky (0.133–0.998); Krasheninnikov (0.134–0.86); Bogoslof (0.093–0.97); Popocatepetl (0.183–0.98); and Java Bajah Dome Miocene (0.334–0.89); Pliocene (0.235–0.82).

resent binary mixing relationships between different end-members. Moreover, all the correlations seem to converge on a similar unradiogenic Os-rich end-member.

Duplicate analyses for half of the samples show that both Os concentrations and isotopic ratios are heterogeneous within samples. The largest ranges observed in a sample for Os concentrations and $^{187}Os/^{188}Os$ initial ratios were respectively 0.530–11.151 ppt (sample A29107, Avachinsky volcano, Kamchatka) and 0.466–0.941 (sample YH18, Hakone volcano, Japan). The Re distribution was much less heterogeneous, but still had a maximum range of 286–646 ppt in sample A29107. When reported on the $^{187}Os/^{188}Os$ versus $1/^{188}Os$ diagrams (Fig. 4), the multiple analyses of a heterogeneous sample are in good agreement (with the exception of two samples, B1796, Bogoslof, Aleutians and P33182, Tolbachik, Kamchatka) with the mixing line defined for the whole set of samples from the same volcano (e.g., samples from St. Vincent island, Lesser Antilles and sam-

ple YH18, Hakone, Japan), or even define themselves a mixing line (651-1, Krasheninnikov, Kamchatka, $r^2 = 0.86$).

4. Discussion

Important variations exist in Re and Os contents and Os isotope ratios of arc lavas. Those variations are observed in subduction zones from all around the world and seem to reflect binary mixing relationships expressed by positive linear correlations between the Os isotopic ratio and the inverse of its concentration.

All the correlations seem to converge on a similar unradiogenic Os-rich end-member (Fig. 4). Yet, the actual regression lines' intercepts display a large range of $^{187}Os/^{188}Os$ values, from 0.013 to 0.334 (except for Saba, Lesser Antilles: −0.132). This range includes upper mantle values, as defined from both MORB glasses [6] and peridotites (e.g.,[15]), and may indicate Os isotope heterogeneity of the depleted part of the mantle wedge, due, for example, to different metasomatism histories. However, this explanation should be taken with caution because the range in the unradiogenic component signature likely results only from poor determination of the origin of the mixing lines, as illustrated by the meaningless negative intercept for Saba. Because the study of the mantle wedge composition is beyond the scope of this paper, the unradiogenic component will, from here, be taken to represent the mantle wedge, regardless of its possible Os isotopic heterogeneity.

In this section, we will discuss the nature of materials, which can possibly represent the Os radiogenic components identified in arc lavas. These materials, and the processes by which they impart their signatures to lavas, must account for: (1) the systematic occurrence of binary mixtures in arc volcanoes from various geodynamic settings; (2) a time-dependent variation in the radiogenic component for a given volcano [7]; (3) the radiogenic signatures of both primitive and differentiated arc lavas; (4) the existence of a variety of Os radiogenic components in subduction-related volcanism; and (5) the heterogeneity in Os concentrations and isotopic ratios of the samples. The two main hypotheses that will be discussed are shallow-level fractionation and contamination of the magmas and heterogeneity of the mantle source due to subducted slab supply.

4.1. Shallow-level processes

The arc lavas analyzed in this study have extremely low Os contents (mostly ≤ 10 ppt) when compared to mantle peridotites. These small concentrations may reflect the compatible behavior of Os during mantle melting. However, since most of the samples are differentiated, fractional crystallization may also play an important role in lava concentrations, although it alone cannot produce the linear relationships displayed in Fig. 4 because isotopes are not fractionated by such a process.

Nevertheless, the effect of fractional crystallization on Os contents is still a matter of debate. As Os is clearly a compatible element in the terrestrial mantle, one would also expect its content in lavas to decrease with increasing silica content and to be concentrated in Fe–Mg minerals. However, recent studies have shown that Os is incompatible in magmatic olivine (from oceanic basalts), as opposed to mantle olivine [16,17]. Consequently, the authors inferred that fractional crystallization alone cannot explain the Os–Mg–Ni variations observed in oceanic basalt, but source heterogeneity or sulfide/olivine parallel crystallization could.

We have thus plotted Os contents as a function of SiO_2, Mg# and Ni contents in Fig. 5. Taken as a whole, the present analyses fail to reveal any clear correlation between Os contents and indices of differentiation such as SiO_2 (Fig. 5a) or La/Yb (not shown). However, for Japan, a negative correlation appears with SiO_2, with the exception of the most Os-rich and silica-rich sample. For Japan and Kamchatka, positive relationships also appear between Os and Ni and Mg#, for the whole arc data set, as well as within each volcano sample set, although it should be noted that in the latter case, such trends are based on two or three samples only. These observations suggest, at least for these arcs, that Os behavior during fractional crystallization is somehow related to that of Ni. However, it must be emphasized that from the

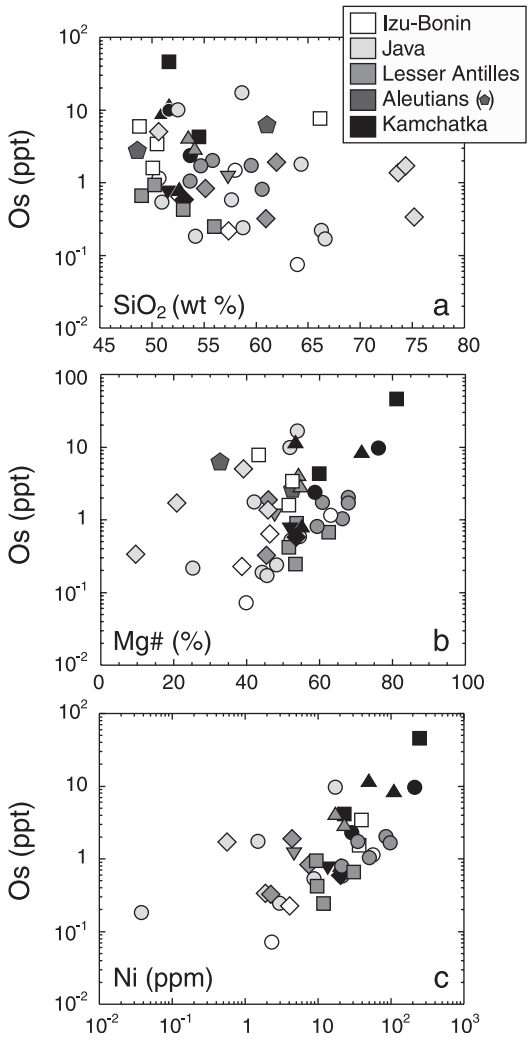

Fig. 5. Os concentrations versus SiO_2 (a), Mg# (b) and Ni (c) contents. Because of sample Os heterogeneity, and for simplicity, we have represented each sample by its average value of Os content to avoid plotting several values of Os for each Ni, SiO_2 or Mg# value. Each arc is represented by a single shade, and for each shade, each shape of symbol is for a different volcano of the same arc.

present data, Os–Ni co-behaviors do not appear to be systematic and that even the most primitive samples (with Mg# higher than 65) have very low concentrations of Os (≤ 10 ppt, except for sample A8501, Kamchatka), which are comparable to those of the differentiated lavas. In addition, the absence of systematic relationships between Os and the degree of differentiation of the rocks (SiO_2, Mg# and La/Yb) suggest a geochemical behavior of osmium, different from that recently inferred for Os-rich rocks from Western Mexico [12], where Os, SiO_2 and MgO contents show a direct relationship.

In summary, it is not clear from our data how osmium is affected by fractional crystallization, although the low contents in the lavas may be partly due to this process.

Alternatively, due to these low Os concentrations, arc lavas are potentially sensitive to contamination and therefore, radiogenic Os isotope ratios of arc lavas and the mixing trends observed for each volcano could reflect a systematic contamination process during arc magma ascent (interaction with and/or assimilation of the crustal basement, e.g., [12,18,19]) or after eruption (hydrothermalism, e.g., [19]).

Oceanic or continental crusts on which arcs are built are likely to be very radiogenic and could in fact affect the signature of the magma and possibly create the observed rock heterogeneity. In addition, the nature, age and thickness of these basements, from one zone to another, are very variable and can explain the range of isotopic signatures observed for the radiogenic component of the mixing trends.

On the other hand, contamination via assimilation of crustal basement is usually invoked when volcanoes are built on continental crust or thick layers of sediments [12,18,20]. In fact, the thermodynamic conditions and effect of assimilation of continental crust materials on the chemical composition of magmas have been well studied through the so-called assimilation–fractional crystallization model (AFC, e.g., [21,22]), but the case of oceanic crust assimilation has rarely been considered. Nevertheless, among the subduction zones represented in Fig. 4, only Mount Fuji, Japan, Popocatepetl, Mexico, and Martinique, Lesser Antilles lie on continental or sedimentary basements, while the Izu–Bonin arc, the Lesser Antilles, and the Aleutians are oceanic arcs (Table 1). Yet, we observe mixing lines for all volcanoes, regardless of the nature of the basement, and we have not found any relationship between the slope of the mixing line or the range of Os ratios for a given volcano and the nature,

thickness or age of the overlying plate, as could be expected for simple contamination via basement assimilation.

Moreover, even though assimilation of continental crust (and oceanic crust) would strongly affect, through partial melting, the incompatible element contents of arc basalts, it is less clear what the effect is on a compatible element such as Os, which is likely to be very radiogenic but also very depleted in crustal materials. One could thus expect that compatible elements are significantly less involved in the assimilation process. Yet, as mentioned above, the studied samples display very typical arc lava patterns in Fig. 1, which show no evidence of secondary enrichment from crustal material.

Finally, the linear relationships between Os isotopes and the inverse of Os concentrations could be explained by a constant assimilation/differentiation ratio (AFC model). This would further imply that the Os concentrations and isotope ratios of arc lavas decrease with increasing degree of differentiation of the rocks. However, as already mentioned, no clear relationship exists between Os and differentiation indices (SiO_2, Mg# (Fig. 5a,b), and trace elements) for the samples analyzed (except, to some extent, for Os contents in Japan and Kamchatka, but it is not true for Os isotope ratios (not shown)) and primitive arc lavas from Kamchatka show mixing lines and radiogenic Os ratios similar to the ones for the more silica-rich arc samples analyzed in this study (cf. Fig. 4c).

In the case of Java [7], contamination by basement rocks was dismissed for this reason and also because it was hard to reconcile with the two radically different mixing trends defined by Miocene and Pliocene samples of the single Bajah volcanic dome of Java, especially because it would imply that osmium isotopic characteristics of the basement have strongly changed with time.

Os mobility has been observed in hydrothermal systems of mid-ocean ridge settings [23], and hydrothermal contamination after eruption has been invoked to explain some highly radiogenic signatures of oceanic basalts [24] via secondary post-entrapment alteration by seawater-derived radiogenic Os. Moreover, Brenan et al. [19] call attention to the fact that hydrothermalism may be a significant process overprinting initial Os isotope ratios of lavas, because of the low closure temperature of pyrrhotite and possibly other Os-rich sulfide or oxide phases. However, as for the assimilation hypotheses, it is unlikely that hydrothermal events occurred systematically in all the areas we looked at, regardless of the particular setting of each zone.

In summary, although some arc magmas are contaminated by the crustal basement they travel through (as shown by their trace element and Sr, O, Nd or Pb isotope signatures), and differentiated magmas are more likely to be exposed to such a process, it seems unlikely that the high Os isotope ratios measured in arc lavas presented here and the systematic observation of Os isotope mixing lines for a set of worldwide subduction-related volcanoes can be explained by this single process. The lack of understanding of Os behavior during both crystallization and partial melting of basement wall rocks in contact with hot magma makes it difficult at present to discuss more precisely this hypothesis, and we believe that further investigation is needed to assess its effects on Os contents of lavas.

4.2. Mantle source heterogeneity

An alternative explanation for the Os characteristics of arc lavas is that the mixing lines documented in this study reflect mixtures, in the source, of Os from the mantle and from the slab. In this case, the unradiogenic components can be accounted for by the mantle wedge and the radiogenic components may be either the altered oceanic crust and/or the sediments that are subducted beneath the arc. A similar hypothesis has been proposed for the Miocene and Pliocene trends defined by samples from Bajah Volcano from Java [7], mainly because each of these trends was formed by samples having a distinct and homogeneous Pb signature, MORB-like Pb isotope ratios for Miocene samples and sediment-like Pb ratios for Pliocene samples.

Sediments have $^{187}Os/^{188}Os$ isotope ratios of about 1 and 1.3, for marine and terrigenous sediments respectively (e.g., [8]). These high values are

in good agreement with the radiogenic end-members of some of the mixing lines (for example, St. Vincent, St. Kitts, or the Kamchatka trends). However, sediments alone cannot account for all the trends we have determined, especially those that have isotopic ratios similar to or even higher than those of sediments (Mt. Hakone in Japan, Martinique and Saba in the Antilles, Miocene lavas in Java). Moreover, in the case of Kamchatka, previously published Pb isotope data seem to exclude sediments as a significant component of the magma source (e.g., [25]).

The oceanic crust subducting at the trenches of the considered subduction zones has high $^{187}Re/^{188}Os$ ratios (based on MORB values from [6]) with a range of ages from 15 to 150 Ma. Consequently, the subducted crust must be much more radiogenic than the mantle wedge rocks and therefore gives a potential end-member for the observed trends of Fig. 4. For example in Java, where the highest Os isotope ratios were measured, an estimate of the oceanic crust Os ratio gives a value of 6 for the $^{187}Os/^{188}Os$ ratio [7], which is much higher than the highest ratio measured in an arc lava (3.15 [7]). Moreover, it is a priori different for each subduction zone depending on the age and $^{187}Re/^{188}Os$ ratio of the crust. Yet, Re and Os behaviors during hydrothermalism at ridges and during metamorphic processes are poorly understood and the $^{187}Re/^{188}Os$ ratio of the subducting slab may be quite different from the ratios measured in MORB. Eclogites and blueschists, which are thought to be the result of metamorphism of the oceanic crust during subduction, have similar Os concentrations and significantly lower Re concentrations when compared to MORB [26]. In this case, calculated values for the Os isotope ratio of altered oceanic crust may be overestimated when using $^{187}Re/^{188}Os$ values of MORB. However, Becker [26] suggested that Re is more likely removed from the oceanic crust during the subduction metamorphism itself, rather than during hydrothermalism at ridges. In this case, the oceanic crust can develop very high Os isotope ratios by radio-decay of Re during its transport to the trench, before releasing Re in larger amounts than Os in the subduction zone.

Applying the calculation adopted for Java samples to the other subduction zones (taking into account the respective ages of the crust and the average $^{187}Re/^{188}Os$ ratios of MORB for the given ocean [6]), we obtain, in the case of Izu–Bonin, Kamchatka, the Lesser Antilles, the Aleutians, and Mexico, $^{187}Os/^{188}Os$ ratios of 13, 8, 1.4, 5 and 1.4 respectively, for the subducting oceanic crust. These values are all higher than the more radiogenic arc lava from the same region, except for the Lesser Antilles, where one sample is slightly more radiogenic than the estimated down-going oceanic crust. Therefore, adding radiogenic Os from the subducted oceanic crust to the mantle wedge appears to be a potential way to explain the binary mixtures observed for each volcano. As $^{187}Re/^{188}Os$ ratios have been shown to be quite variable along a single ridge [6], for the Lesser Antilles, the calculated altered oceanic crust $^{187}Os/^{188}Os$ ratio (considering the average $^{187}Re/^{188}Os$ value for the Atlantic MORB) may be lower than the actual ratio of the crust beneath the Lesser Antilles arc.

However, the case of Java shows that the crust alone cannot explain the existence of two linear trends for the Miocene and the Pliocene samples from this volcano because it would imply either an important change in the mobilization of radiogenic Os or that the crust subducted below the volcanic dome did not have the same isotopic signature during the Miocene and Pliocene. Moreover, some regions, Java, and also the Lesser Antilles, clearly display sediment-like signatures for Sr, Nd and Pb isotopes (e.g., [1,27]), and thus the role of sediments in their Os signatures should be considered.

Combining oceanic crust and subducted sediments in the magma source could be another way to explain the unique characteristics of the source of each volcano [7]. Unfortunately, the lack of constraints on the actual Os isotope characteristics of the subducting materials at each particular trench and Os partition coefficients during partial melting of metasomatized sources and slab dehydrating processes makes it difficult at present to quantitatively model the mixing processes. In any case, the observations suggest that a three-component mixture could occur in the melting

zone, between the depleted upper mantle rocks and variable proportions of oceanic crust and sediments, a hypothesis supported by previous arc studies (e.g., [2,28]). Furthermore, the linearity of the trends obtained in the $^{187}Os/^{188}Os$ versus $1/^{188}Os$ diagram suggests that the ratio of recycled sediments to oceanic crust contributions is constant for a given volcano at a given period of time. The slab-derived H_2O-rich component is believed to induce mantle melting at mantle wedge temperatures, by lowering the peridotite solidus (e.g., [29]). The Os results further suggest that the radiogenic slab component, made of sediment-derived and oceanic crust-derived materials, was homogenized before initiating mantle melting. A similar conclusion has been reached based on boron and beryllium contents [28], and boron isotope [3] data on arc lavas. We must note, however, that unlike our results, these studies infer that the homogeneous subducted component made from oceanic crust and sediments contributions is unique for a whole arc [28] or across an arc from the volcanic front to the back-arc [3].

Although source heterogeneity can account for the observed Os characteristics in arc lavas, it raises a few questions, which can be summarized as follows.

First, it has not been possible so far to observe any covariation between Os and either other subduction contributions or mantle melting indices in our data, which would confirm the deep origin of Os signatures. This is likely due to the effect of later fractional crystallization on the trace element contents of the fractionated rocks.

Second, the respective proportions of oceanic crust and sedimentary Os cannot be the only factors responsible for the slope of the mixing line. Indeed, in that case, the Lesser Antilles arc should show decreasing slopes from northern to central islands, because of the increasing thickness of the sediment column in the Lesser Antilles trench (e.g., [30]). Yet, this is not the case (cf. St. Kitts and Saba, Fig. 4). A possible explanation may be modification of the original Os contents by fractional crystallization, without destroying the mixing trends, but fractional crystallization more likely accounts only for scatter in some trends. Another explanation for the varying mixing lines of the islands along the Lesser Antilles arc may be along-arc $^{187}Re/^{188}Os$ ratio heterogeneity of the oceanic and/or different partition coefficients for Os from one volcano source to another depending on the slab physical parameters or on slab water contents.

Another point is the possibility of preserving these source characteristics through magma ascent in the mantle and in the arc basement before reaching the surface. Not only arc lavas but also HIMU OIB have radiogenic Os signatures which may be interpreted as originating from crust recycling in the mantle melting zone [4,5]. Several disequilibrium hypotheses have been proposed to allow these magmas to reach the surface without having equilibrated with unradiogenic Os-rich mantle peridotites, including shielding of mantle Os in Os-rich phases within host minerals [31], slow equilibration kinetics between peridotites and melts [26], isolation of melts from peridotites by reaction zones along conduit walls [26], and rapid ascent through a network of channels [4].

Finally, another disequilibrium state, which is inferred from arc lavas, is sample heterogeneity for Os contents and isotope ratios. Such heterogeneity has also been observed in mantle rocks and OIB (e.g., [15]), and led, for mantle rocks, to the 'nugget effect' hypothesis, which is a preferential distribution of Os in refractory sulfide or oxide micro-inclusions. These Os-bearing phases may be in isotopic disequilibrium with their host minerals, suggesting that diffusion processes between the inclusion and the host mineral have been prevented [31]. For lavas, the observed heterogeneity implies that the magmas themselves are heterogeneous in concentration and isotopic composition, and that they are not homogenized during ascent to the surface. Although such a process is not well constrained at present, Os heterogeneity of the samples suggests that the radiogenic Os transferred from lithospheric fluids or melts cannot equilibrate, within the arc magmas, with the unradiogenic Os coming from the mantle.

Acknowledgements

The authors wish to thank R. Maury, M. Se-

met, I. Kaneoka, J.-L. Joron and J.-C. Komorowski for providing most of the samples. We are very grateful to J.-L. Birck for technical assistance in measuring Os concentrations and isotope ratios. We also thank K. Burton and B. Bourdon for profitable discussions, and P. Foster for careful reading and improving of the manuscript. C. Hawkesworth and an anonymous reviewer are also thanked for their thorough reviews. This work was largely supported by a grant from the Bureau de Recherches Géologiques et Minières (BRGM) to S.A.*[BW]*

References

[1] D. BenOthman, W.M. White, P.J. Patchett, The geochemistry of marine sediments, island arc magma genesis and crust-mantle recycling, Earth Planet. Sci. Lett. 94 (1989) 1–21.

[2] C.J. Hawkesworth, S.P. Turner, F. McDermott, D.W. Peate, P. van Calsteren, U-Th isotopes in arc magmas: Implications for element transfer from the subducted crust, Science 276 (1997) 551–555.

[3] T. Ishikawa, E. Nakamura, Origin of the slab component in arc lavas from across-arc variation of B and Pb isotopes, Nature 370 (1994) 205–208.

[4] E.H. Hauri, S.R. Hart, Re-Os isotope systematics of HIMU and EMII oceanic island basalts from the South Pacific Ocean, Earth Planet. Sci. Lett. 114 (1993) 353–371.

[5] P. Schiano, K.W. Burton, B. Dupré, J.L. Birck, G. Guille, C.J. Allègre, Correlated Os-Pb-Nd-Sr isotopes in the Austral-Cook chain basalts: The nature of the mantle components in plume sources, Earth Planet. Sci. Lett. 186 (2001) 527–537.

[6] P. Schiano, J.-L. Birck, C.J. Allègre, Osmium-strontium-neodymium-lead isotopic covariations in mid-ocean ridge basalt glasses and the heterogeneity of the upper mantle, Earth Planet. Sci. Lett. 150 (1997) 363–381.

[7] S. Alves, P. Schiano, C.J. Allègre, Rhenium-osmium isotopic investigation of Java subduction zone lavas, Earth Planet. Sci. Lett. 168 (1999) 65–77.

[8] B. Peucker-Ehrenbrink, G. Ravizza, A.W. Hofmann, The marine $^{187}Os/^{186}Os$ record of the past 80 million years, Earth Planet. Sci. Lett. 130 (1995) 155–167.

[9] T. Meisel, R.J. Walker, J.W. Morgan, The osmium isotopic composition of the Earth's primitive upper mantle, Nature 383 (1996) 517–520.

[10] B.K. Esser, K.K. Turekian, The osmium isotopic composition of the continental crust, Geochim. Cosmochim. Acta 57 (1993) 3093–3104.

[11] L.E. Borg, A.D. Brandon, M.A. Clynne, W.J. Walker, Re-Os isotopic systematics of primitive lavas from the Lassen region of the Cascade arc, California, Earth Planet. Sci. Lett. 177 (2000) 301–317.

[12] J.C. Lassiter, J.F. Luhr, Osmium abundance and isotope variations in mafic Mexican volcanic rocks: Evidence for crustal contamination and constraints on the geochemical behavior of osmium during partial melting and fractional crystallization, Geochem. Geophys. Geosyst. 2 (2001) 2000GC000116.

[13] J.-L. Birck, M. Roy-Barman, F. Capmas, Re-Os isotopic measurements at the femtomole level in natural samples, Geostand. Newslett. 20 (1) (1997) 19–27.

[14] J.L. Birck, C.J. Allègre, Contrasting Re/Os magmatic fractionation in planetary basalts, Earth Planet. Sci. Lett. 124 (1994) 139–148.

[15] S.R. Hart, G. Ravizza, Os partitioning between phases in lherzolite and basalt, in: A. Basu, S.R. Hart (Eds.), Earth Processes: Reading the Isotopic Code, Am. Geophys. Union, Washington, DC, 1996, pp. 123–134.

[16] K.W. Burton, P. Schiano, A. Gannoun, J.-L. Birck, C.J. Allègre, Contrasting behaviour of osmium in mantle and magmatic olivine, in: Fall Meeting, EOS Trans. AGU, San Francisco, CA, 2000.

[17] J.M. Brenan, W.F. McDonough, I. Horn, P. Sattari, Olivine-melt partitioning of Re and the PGEs: Experimental constraints, in: Spring Meeting, EOS Trans. AGU, 2000.

[18] J.P. Davidson, Crustal contamination versus subduction zone enrichment: Examples from the Lesser Antilles and implications for mantle source compositions of island arc volcanic rocks, Geochim. Cosmochim. Acta 51 (1987) 2185–2198.

[19] J.M. Brenan, D.J. Cherniak, L.A. Rose, Diffusion of osmium in pyrrhotite and pyrite: implications for closure of the Re-Os isotopic system, Earth Planet. Sci. Lett. 180 (2000) 399–413.

[20] W. Hildreth, S. Moorbath, Crustal contributions to arc magmatism in the Andes of Central Chile, Contrib. Mineral. Petrol. 98 (1988) 455–489.

[21] D.J. DePaolo, Trace element and isotopic effects of combined wall rock assimilation and fractional crystallization, Earth Planet. Sci. Lett. 53 (1981) 189–202.

[22] W.A. Bohrson, F.J. Spera, Energy-constrained open-system magmatic processes II: Application of energy-constrained assimilation-fractional crystallization (EC-AFC) model to magmatic systems, J. Petrol. 42 (2001) 1019–1041.

[23] G.E. Brügmann, P. Herzig, A.W. Hofmann, Os isotopic composition and Os and Re distribution in the active mound of the TAG-hydrothermal system, Mid-Atlantic Ridge, Proc. ODP Sci. Results 158 (1998) 91–100.

[24] F. Marcantonio, A. Zindler, T. Elliott, H. Staudigel, Os isotope systematics of La Palma, Canary Islands: Evidence for recycled crust in the mantle source of HIMU ocean islands, Earth Planet. Sci. Lett. 133 (1995) 397–410.

[25] A.B. Kersting, R.J. Arculus, Pb isotope composition of Klyuchevskoy volcano, Kamchatka and North Pacific sediments: Implications for magma genesis and crustal

recycling in the Kamchatkan arc, Earth Planet. Sci. Lett. 136 (1995) 133–148.
[26] H. Becker, Re-Os fractionation in eclogites and blueschists and the implications for recycling of oceanic crust into the mantle, Earth Planet. Sci. Lett. 177 (2000) 287–300.
[27] J.P. Davidson, Lesser Antilles isotopic evidence of the role of subducted sediment in island arc magma genesis, Nature 306 (1983) 253–256.
[28] J.D. Morris, W.P. Leeman, F. Tera, The subducted component in island arc lavas: Constraints from Be isotopes and B-Be systematics, Nature 344 (1990) 31–36.
[29] E. Stolper, S. Newman, The role of water in the petrogenesis of Mariana trough magmas, Earth Planet. Sci. Lett. 121 (1994) 293–325.
[30] R.C. Maury, G.K. Westbrook, P.E. Baker, P. Bouysse, D. Westercamp, Geology of the Lesser Antilles, in: G. Deng, J.E. Case (Eds.), The Geology of North America, H, The Caribbean Region, Geol. Soc. Am., Boulder, CO, 1990, pp. 141–165.
[31] K.W. Burton, P. Schiano, J.-L. Birck, C.J. Allègre, Osmium isotope disequilibrium between mantle minerals in a spinel-lherzolite, Earth Planet. Sci. Lett. 172 (1999) 311–322.
[32] S.S. Sun, W.F. McDonough, Chemical and isotopic systematics of oceanic basalts: Implications for mantle composition and processes, in: A.D. Saunders, M.J. Norry (Eds.), Magmatism in the Ocean Basins, Vol. 42, Geol. Soc., Blackwell Scientific, Oxford, 1989, pp. 313–345.
[33] A.W. Hofmann, Chemical differentiation of the Earth: The relationship between mantle, continental crust, and oceanic crust, Earth Planet. Sci. Lett. 90 (1988) 297–314.
[34] J. Gill, Orogenic Andesites and Plate Tectonics, Springer-Verlag, Berlin, 1981, 390 pp.
[35] J.W. Curtis, Plate tectonics of the Papua New Guinea-Solomon Islands region, J. Geol. Soc. Aust. 20 (1973) 21–36.
[36] T.A. Plank, C.H. Langmuir, The chemical composition of subducting sediment and its consequences for the crust and mantle, Chem. Geol. 145 (1998) 325–394.
[37] R.D. Jarrard, Relations among subduction parameters, Rev. Geophys. 24 (1986) 217–284.
[38] G.K. Westbrook, Magnetic lineations and fracture zones, in: R.C. Speed, G.K. Westbrook (Eds.), Lesser Antilles Arc and Adjacent Terranes: Ocean Margin Drilling Program Regional Atlas Series, Marine Science International, Woods Hole, MA, 1984, Sheet 5.
[39] A.S. Furumoto, J.P. Webb, M.E. Odegard, D.M. Hussong, Seismic studies on the Ontong Java Plateau, Tectonophysics 34 (1976) 71–90.
[40] D.M. Finlayson, J.P. Cull, Structural profiles in the New Britain-New Ireland region, J. Geol. Soc. Aust. 20 (1973) 37–48.
[41] W.B. Hamilton, Tectonics of the Indonesian Region, U.S. Geol. Surv. Prof. Paper, 1979, 345 pp.
[42] T. Matsuda, Collision of the Izu-Bonin arc with central Honshu: Cenozoic tectonics of the Fossa Magna, Japan, in: S. Uyeda, R.W. Murphy, K. Kobayashi (Eds.), Geodynamics of the Western Pacific, Advances in Earth and Planetary Sciences, Vol. 6, Japan Scientific Societies Press, Tokyo, 1979, pp. 409–421.
[43] B.F. Watson, K. Fujita, Tectonic evolution of Kamchatka and the Sea of Okhotsk and implications for the Pacific Basin, in: D.G. Howell (Ed.), Tectonostratigraphic Terranes, Circum-Pacific Council for Energy and Mineral Resources, Houston, TX, 1985, pp. 333–348.
[44] E. Heath, S.P. Turner, R. Macdonald, C.J. Hawkesworth, P. van Calsteren, Long magma residence times at island arc volcano (Soufrière, St. Vincent) in the Lesser Antilles Evidence from ^{238}U-^{230}Th isochron dating, Earth Planet. Sci. Lett. 160 (1998) 49–63.
[45] F. Pineau, M.P. Semet, N. Grassineau, V.M. Okrugin, M. Javoy, The genesis of the stable isotope (O, H) record in arc magmas: The Kamchatka's case, Chem. Geol. 153 (1999) 93–124.
[46] M. Tatsumoto, R.J. Knight, Isotopic composition of lead in volcanic rocks from central Honshu – with regard to basalt genesis, Geochem. J. 3 (1969) 53–86.
[47] R.W. Johnson, D.A. Wallace, D.J. Ellis, Feldspathoid-bearing potassic rocks and associated types from volcanic islands off the coast of New Ireland Papua New Guinea: A preliminary account of geology and petrology, in: R.D. Johnson (Ed.), Volcanism in Australia, Elsevier, Amsterdam, 1976.
[48] M. Lindner, D.A. Leich, G.P. Russ, J.M. Bazan, R.J. Borg, Direct determination of the half-life of ^{187}Re, Geochim. Cosmochim. Acta 53 (1989) 1597–1606.
[49] M.T. McCulloch, M.R. Perfit, $^{143}Nd/^{144}Nd$, $^{87}Sr/^{86}Sr$ and trace element constraints on the petrogenesis of Aleutian island arc magmas, Earth Planet. Sci. Lett. 56 (1981) 167–179.
[50] M. Roy-Barman, Mesure du rapport $^{187}Os/^{186}Os$ dans les basaltes et péridotites: Contribution à la systématique $^{187}Re/^{186}Os$ dans le manteau, Thèse en Géochimie, Université Denis Diderot, Paris VII, 1993.